High-symmetry low-energy structures of $C_{60}H_{60}$ and related fullerenes and nanotubes

Aristides D. Zdetsis
Department of Physics, University of Patras, GR-26500 Patras, Greece
(Received 7 November 2007; revised manuscript received 28 January 2008; published 4 March 2008)

The structure, symmetry, and stability of $C_{60}H_{60}$ are studied by *ab initio* density functional theory and second order Møller-Plesset perturbation theory. It is shown that the lowest energy high symmetry (D_{5d}) cage of $C_{60}H_{60}$ is obtained by "puckering" of the H-C-C-H bonds through the endohydral bonding of ten C-H pairs of the full icosahedral fullerene. Such puckering can also lead to alternative D_{5d} symmetric structures and to other partially hydrogenated fullerenes which have been already synthesized as well as to single wall carbon nanotubes. The infrared spectrum of the proposed structure(s) is compatible with analogous astronomical data on the basis of which the existence of $C_{60}H_{60}$ in stellar atmospheres was postulated.

DOI: 10.1103/PhysRevB.77.115402 PACS number(s): 31.90.+s, 61.46.Fg, 61.46.Bc, 81.05.Tp

I. INTRODUCTION

The discovery of buckminsterfullerene (C_{60}) and other related substances stimulated a lot of interest in their use (among others) as substrates for addition reactions such as hydrogenation. Attempts to synthesize the fully hydrogenated $C_{60}H_{60}$ fullerene (with perfect icosahedral symmetry) have failed so far, although its existence in stellar atmospheres was postulated since 1991[1] through comparison of the observed spectral lines with semiempirical calculated infrared (IR) spectra. Instead, partially hydrogenated cages of the form $C_{60}H_n$, with n up to 36 have been synthesized.[2,3] The only fully hydrogenated fullerene which has been synthesized up to now is dodecahedrane,[4] $C_{20}H_{20}$, while cubane C_8H_8, the smallest fully hydrogenated cage with octahedral symmetry, was synthesized as early as 1964,[5] much earlier than the discovery of fullerenes. The purpose of the present work is the study of the fullerene $C_{60}H_{60}$ and a reexamination of its structure and stability in view of earlier work[6(a)] suggesting a C_1-symmetric (nonsymmetrical) isomer as the ground state of $C_{60}H_{60}$ (see also Ref. 3, p. 4175). Other early attempts to relieve the strains imposed by the high icosahedral symmetry by partially distorting the I_h to I symmetry[6(b)] (in particular, for $C_{60}F_{60}$ and by extension to $C_{60}H_{60}$) were rather unsuccessful, since the I-symmetric structure was eventually found less stable compared to the icosahedral structure.[6(c)] Thus, although the I-symmetry was very attractive, preserving the 60-fold equivalence of F (or H) and C nuclei (giving a chiral equilibrium structure[6(b)]), the nonsymmetric C_1 structure is more stable than both I_h and I-symmetric structures.[3,6(a),6(c)]

This C_1 isomer has ten hydrogen atoms inside the cage so as to allow each H-C-C-H fragment, corresponding to a C-C shared edge, to adopt a chairlike structure with one hydrogen atom pointing inside the cage and one pointing outward.[4,6] This allows optimization of the sp^3 bonding. Although such a structure is found lower in energy,[6] it has the drawback of lack of symmetry and favorable comparison with astronomical IR data, as the fully symmetric I_h isomer. However, between these two extremes there should be (as almost always) a "happy medium," which would be lower in energy and closer to the aesthetically and scientifically more appealing icosahedral symmetry. In the current work, the search for a low-energy high-symmetry alternative of the icosahedral $C_{60}H_{60}$ cage leads to a structure of high D_{5d} symmetry with much lower energy than the C_1 structure. This and other alternative structures of similar symmetry are discussed below in Sec. III, after the short description of some technical details in Sec. II. Finally, a summary with the important conclusions of the present work is given in Sec. IV.

II. SOME TECHNICAL DETAILS OF THE CALCULATIONS

The general theoretical and computational method followed for all clusters and cages is all electrons density functional theory (DFT) with the hybrid, nonlocal exchange and correlation functional of Becke-Lee, Parr, and Yang (B3LYP).[7] The starting geometries were obtained by suitable puckering of the bonds, preserving the D_{5d} symmetry, although the geometry optimizations were run with and without symmetry constraints. The calculations were supplemented with vibrational frequency calculations to obtain the IR spectrum and check at the same time for imaginary frequencies. These calculations were performed with the TURBOMOLE program package[8] using the triple zeta valence polarized (TZVP) basis set.[9] For the lowest-energy structures MP2 calculations were performed (starting from the B3LYP/TZVP geometry) with the same basis sets and program package. Finally, the calculations for the optical absorption-emission spectra were performed in the framework of time-dependent DFT (TDDFT) with a B3LYP functional, as implemented in the TURBOMOLE program package.[8]

III. RESULTS AND DISCUSSION

The lowest-energy highest-symmetry (D_{5d}) structures of $C_{60}H_{60}$ obtained here are shown in Fig. 1. These structures are characterized by D_{5d} symmetry, the largest and simplest subgroup of I_h. The structure in Fig. 1(a) has ten endohedral hydrogen atoms in hexagonal chairlike arrangements with neighboring exohedral hydrogens (similar to the C_1 structure). Furthermore, similar (and more accurately) to the I_h isomer in Fig. 2(c), the IR spectrum of this structure, as will be shown below, reproduces fairly well the stellar data used by Webster[1] to postulate the existence of $C_{60}H_{60}$ in stellar atmospheres. As a first attempt towards a low-energy high-

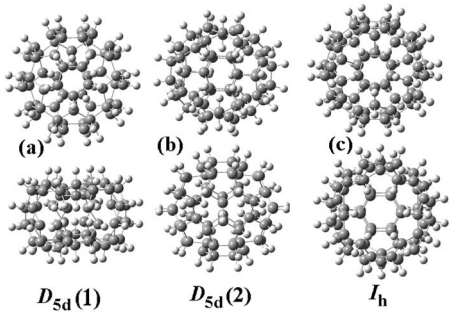

FIG. 1. Lowest-energy (high-symmetry) structures of $C_{60}H_{60}$: top view (top) and side view (bottom). The structures in (a) and (b) are characterized by D_{5d} symmetry and ten endohydral hydrogens. The structure in (c) has full icosahedral symmetry and all hydrogen atoms exohedral.

symmetry isomer this structure is very close to the target. However, the structure in Fig. 1(b), which is also characterized by D_{5d} symmetry, with ten (different) endohedral hydrogen atoms, is even lower in energy, and obviously lower than the full I_h structure in Fig. 2(c). The difference between the two structures is that the endohedral hydrogens are bonded to different sets of carbon atoms belonging to different types of carbon rings. In the structure of Fig. 1(b) the "puckering" of hexagonal (and pentagonal) rings is energetically more favorable compared to the structure of Fig. 1(a) in which more pentagons and fewer hexagons are puckered. Obviously, puckering is favorable for hexagons, where the bond angles of 120° are far away from the ideal sp^3 bond angles (although very close to the sp^2 bond angles), but not for pentagons in which the bond angles are very close to the ideal tetrahedral bond angles. Therefore there is always an energetic compromise involved in puckering. For instance, in $C_{20}H_{20}$, which consists solely of pentagons, the puckering is totally unfavorable. On the contrary, for larger icosahedral fullerenes, Linnolahti *et al.*[10] have shown that puckering leads to very stable fullerenes of equal or even greater stability than $C_{20}H_{20}$. The structure in Fig. 1(b), through better optimization of the puckering (more hexagons than pentagons are hydrogenated endohydrally) is more stable by 0.13 eV per C-H unit than the structure of Fig. 1(a). This is the lowest-energy D_{5d} symmetric structure with all frequencies real, as the structure $D_{5d}(1)$ in Fig. 1(a). Both puckered D_{5d} states would not be easily accessible due to the high-energy barrier for penetration of hydrogen into the cage.

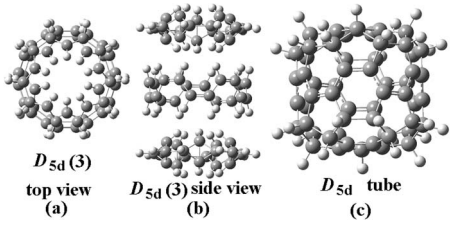

FIG. 2. D_{5d} symmetric cage with 20 endohydral hydrogens after geometry optimization, (a) and (b). The nanotube structure derived by joining the three pieces in (b), together is shown in (c).

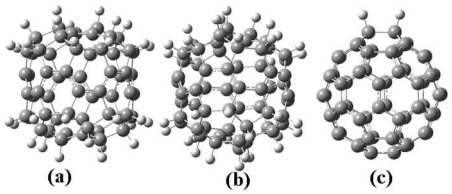

FIG. 3. Partially hydrogenated cages: $C_{60}H_{34}$ (a), $C_{60}H_{36}$ (b), and $C_{60}H_2$ (c).

Therefore, it is possible that they could coexist with the proposed I_h structure.

With fixed D_{5d} symmetry, in addition to the structures of Figs. 1(a) and 1(b), we can also construct very symmetric (D_{5d}) structures with twenty hydrogen atoms pointing inward. Such alternative D_{5d} symmetric structures with 20 endohydral hydrogen atoms turn out to be unstable (with imaginary frequencies). Upon geometry optimization they eventually get separated in three independent $C_{20}H_{20}$ pieces of D_{5d} symmetry each, as is clearly shown in Figs. 2(a) and 2(b).

By removing the intermediate hydrogen atoms and joining the three pieces together we get after optimization the nanotube structure of Fig. 2(c) with the same D_{5d} symmetry. This is a good model for the formation of single wall carbon nanotubes.[11] This "tube" (cage) is practically metallic with a very small gap (about 0.1 eV at the BP86, and 0.3 eV at the B3LYP levels of theory), uneven charge distribution, and very close lying competing singlet and triplet states. The triplet state (at slightly different bond lengths) is the lowest-energy state with a very small energy margin. This is highly suggestive that these states are different manifestations of an open shell singlet state (at about the same energy) which cannot be properly treated with the present theoretical approach. Therefore, the $C_{60}H_{30}$ cage, and cages derived from it, can be considered as the zero-dimensional analog(s) of single wall carbon nanotubes,[11] in which metallic and insulating versions exist, offering a transparent way of understanding the metallicity and the transition from one type of behavior to the other. The tubelike $C_{60}H_{30}$ structure in Fig. 2(c) is not necessarily the lowest-energy structure with this composition. The middle piece can be repeated a large number of times with the two caps at both edges.

To obtain more stable structures we have considered the "excess" charge, which, as Mulliken population analysis shows, is concentrated in four carbon atoms (two on the top and two on the bottom) with no hydrogens attached to them. Two more atoms (one on top and the other on the bottom) have also pronounced charge inequalities but to a lesser degree. By putting initially four, and subsequently, two more (a total of six) hydrogen at these (4+2) carbon atoms we get a more stable $C_{60}H_{34}$ and an even more stable $C_{60}H_{36}$ structure. The $C_{60}H_{34}$ structure is an open shell triplet state, whereas the $C_{60}H_{36}$ cage has a clear highest occupied-lowest unoccupied molecular orbital (HOMO-LUMO) gap of 2.3 eV (at the B3LYP level of theory). These structures are shown in Figs. 3(a) and 3(b). It should be mentioned that $C_{60}H_{36}$ has been synthesized,[3] not necessarily in this particular geometry of Fig. 3(a), and is very stable. The calculated

TABLE I. Binding and cohesive energy HOMO-LUMO gap, together with dominant IR active frequencies (up to four), calculated at the B3LYP level of theory. The frequency of the largest IR intensity is underlined. The structures are identified by the chemical composition (chemical formula), symmetry (sym.), and figure number (Fig.).

Struture/sym. Fig.	E_b (eV/atom)	E_c (ev/atom)	E_g (eV)	ν cm^{-1}
$C_{60}H_{60}$ I_h [1(c)]	9.41	6.83	5.8	1326, 1381, 2946
$C_{60}H_{60}$ D_{5d} [1(a)]	9.46	6.88	6.6	1318, 1410, 2835, 2980
$C_{60}H_{60}$ D_{5d} [1(b)]	9.59	7.01	7.1	2869, 2899, 2929, 2937
$C_{60}H_{60}$ D_{5d} [2(a)]	9.21	6.63	3.6	2984, 2997, 3014, 3145
$C_{60}H_{30}$ D_{5d} [2(c)]	8.23	6.93	(0.4)	1336, 1657, 2850, 2880
$C_{60}H_{34}$ C_{2h} [3(a)]	8.40	6.94	(2.4)	2791, 2825, 2860, 2873
$C_{60}H_{36}$ C_{2h} [3(b)]	8.52	6.98	2.4	2596, 2815, 2826, 2846
$C_{60}H_2$ C_{2v} [3(c)]	6.97	6.88	2.5	1321, 1662, 2863, 2875

(here) optimized structure of $C_{60}H_{36}$ is of C_{2h} (near D_{2h}) symmetry, which although it has the general characteristics and looks very much alike, is not fully identical to either T_h or T-symmetric structures proposed in the literature.[6(c),12] For comparison, the partially hydrogenated $C_{60}H_2$ fullerene is also considered in Fig. 3(c). This fullerene has been synthesized and is very stable too.[3]

To judge and compare the stability of the partially hydrogenated structures in Figs. 2(c) and 3(a)–3(c) on an equivalent basis with the fully hydrogenated fullerenes, we make use of the cohesive energy E_{coh}, instead of the binding energy BE. The cohesive energy E_{coh}, which depends on the structure's size, is defined by the relation

$$E_{coh} = [BE(C_{N_c}H_{N_H}) + \mu_H N_H]/N_C,$$

where $BE(C_{N_c}H_{N_H})$ is the binding (or atomization) energy of the $C_{N_c}H_{N_H}$ cage or nanotube. N_C, N_H are the numbers of C and H atoms, respectively, and μ_H is the chemical potential of H, which is taken at a constant value, with zero corresponding to the value at which the formation energy of methane (CH_4) is zero. Doing so, we have effectively removed the energy contribution of all C-H bonds in every system and essentially considered the binding energy of the "carbon skeleton." This is a common method for the calculation of the cohesive energy.[13] Alternatively, we could have used the "formation energy" which involves the chemical potential of carbon, μ_C, as an additional term without altering the relative energy separations and comparisons between different cages. The cohesive energy together with the binding energy per carbon atom, $E_b = BE(C_{N_c}H_{N_H})/N_C$, and the HOMO-LUMO energy gap E_g are given in Table I for each of the structures studied here. As we can see in Table I, with the exception of the disjoint structure of Figs. 2(a) and 2(b) consisting of three separate pieces, all puckered and partially hydrogenated cages (and "tubes") in the table are more stable compared to the icosahedral (totally exohydrally hydrogenated) $C_{60}H_{60}$ cage. The most stable structure is the D_{5d} symmetric puckered $C_{60}H_{60}$ fullerene of Fig. 1(b), which is even more stable (on the basis of cohesive energy) than structures already synthesized. It would be reasonable therefore to assume that it can be synthesized as well. This fullerene is also characterized by the largest HOMO-LUMO gap which is a zeroth-order measure of "chemical hardness." Since it is also more stable than the C_1 structure with the ten endohydral hydrogen suggested earlier by Sounders[3,6(a)] and Thiel,[6(c)] and since it does not change by totally unconstrained (C_1) optimization, it could be considered as the best candidate for the global minimum of $C_{60}H_{60}$. Yet, independent of its appealing high symmetry, this structure (with so many atoms and open possible combinations) is impossible to be proven or even speculated with confidence as a real global minimum. However, in view of earlier work suggesting that $C_{60}H_{60}$ cages with ten hydrogen atoms pointing inwards are the most stable,[3,6(a)] it is much safer to assume that among all $C_{60}H_{60}$ cages with ten endohydral hydrogen atoms the puckered structure of Fig. 1(b) would be the most stable (and certainly much more stable than the full I_h $C_{60}H_{60}$ fullerene with all hydrogen atoms pointing outwards).

It is interesting to compare the two structures of highest stability, of Fig. 1(b), and highest symmetry, of Fig. 1(c) in other respects besides stability. The IR spectrum is the best choice due to its utilization in the work of Webster[1] for the identification of $C_{60}H_{60}$ in stellar atmospheres, based on unknown origin astronomical IR emission features. To this end, some representative high intensity IR frequencies in the region of 1298 cm^{-1} ($\lambda = 7.7$ nm) and in the range of 2800-3150 cm^{-1} are included in Table I, and the full IR spectrum of these two (and two other related) structures is given in Fig. 4. The frequency at 1298 cm^{-1} (wavelength $\lambda = 7.7$ nm) corresponds to the highest intensity observed in the "unidentified" stellar IR lines. This vibrational mode which is dominated by the bending of the C-C-H bond angles was found with the highest intensity by Webster using a force-field model. With the present B3LYP calculations, this mode, although of relatively high intensity, is not the strongest intensity feature for none of the structures of Table I. Only for three of the structures of Table I, bending modes in this frequency range are among the top four in intensity (listed in Table I).

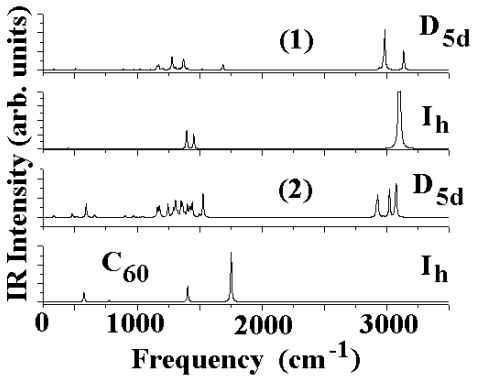

FIG. 4. The calculated IR spectrum of (from top to bottom) $C_{60}H_{60}$ in D_{5d} (a), I_h, and D_{5d} (b) (best energy) symmetries, together with C_{60} (I_h symmetry) for comparison.

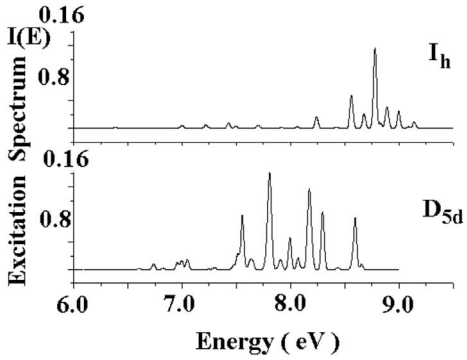

FIG. 5. The calculated optical (emission) spectrum for the I_h and best D_{5d} structures of Figs. 1(b) and 1(c), respectively.

The maximum intensity found by Webster for this mode must be some sort of deficiency of his empirical model. This was verified here by a semiempirical AM1 calculation for the icosahedral $C_{60}H_{60}$ isomer which similarly yields the highest intensity for such a mode at 1287 cm^{-1}. Furthermore, MNDO calculations[6(c)] [see Table 5 in Ref. 6(c)] for the I_h structure give the strongest IR mode at 3145 cm^{-1}, in good agreement to the scaled B3LYP value obtained here (and in disagreement with Webster[1]). For the lowest-energy $C_{60}H_{60}$ structure in Fig. 1(b) this mode is one order of magnitude weaker compared to the peak intensity mode at 2937 cm^{-1}. This particular mode is dominated by the stretching of the ten C-H bonds pointing inward to the cage. The value of 2937 cm^{-1} (like the rest of the frequencies in Table I) has been scaled down by 5% from the calculated B3LYP value of 3092 cm^{-1}. This scaling is a common practice to account for known systematic errors due to fundamental ("one-body" and harmonic) and secondary (technical) approximations, such as the choice of basis sets. Thus, the choice of the scaling factor in reality depends on the level of theory and the basis set.[14] It should be noticed that the 3092 cm^{-1} unscaled value is very close to the observed stellar IR feature at 3050 cm^{-1} ($\lambda = 3.28$ nm), which is the best studied unidentified stellar feature[1] thus far. Webster[1] has concluded that such a mode would be unlikely to be due to C-H stretching in any aliphatic hydrocarbon due to its very short wavelength. Similar conclusions were reached by Linnolahti.[10] Instead, such a mode should be attributed, according to Webster, to lightly hydrogenated fullerenes. From the results of Table I we can see, at least for the partially hydrogenated fullerenes examined here, that this hypothesis is not substantiated, except perhaps for the disjoint pieces of the structure(s) in Figs. 2(a) and 2(b). In this particular case the value of 3145 cm^{-1} is associated with the C-H bond stretching of the outer pieces, whereas the analogous mode of the central piece produces the line at 2997 cm^{-1}. However, this structure is not stable. It seems therefore more likely that the frequency at 3050 cm^{-1} could be associated with C-H bond stretching of the endohydrally bonded hydrogens in the puckered structure of Fig. 1(b). The rest of the relatively high intensity lines in Table I correspond to the observed IR plateau in the range between 2800 and 3100 cm^{-1}, with peak lines at 2800, 2850, 2890, 2940, and 3050 cm^{-1}. From the frequencies listed in Table I, taking also into account the uncertainties in the frequency calculations (and even more so the uncertainties of the corresponding intensities) we can see that the unidentified IR features cannot be safely used to identify uniquely a single source. Almost all of the structures in Table I (and many more not included in the table) produce IR lines in the plateau range and the region of 1300 cm^{-1}. It is more natural to assume, as Webster has suggested, that the IR astronomical data are due to a mixture of (similar?) sources, which are more likely to be associated with fully and partially hydrogenated fullerenes. Concerning the fully hydrogenated fullerenes, we can see that all three stable structures of Fig. 1 are in one way or the other consistent with the IR astronomical features, which cannot be safely used to fully identify the structures. To help further possible identification in the future, the optical excitation spectrum for the icosahedral and the best D_{5d} structure of Fig. 1(b), calculated with the TDDFT method, is shown in Fig. 5. This spectrum was obtained by Gaussian broadening (width 0.001 eV) of the calculated spectral lines. It is clear from this figure that if $C_{60}H_{60}$ is synthesized this spectrum could be used to clearly distinguish between these two key structures.

IV. CONCLUSIONS

It has been illustrated that puckering of the H-C-C-H bonds can lead to much more stable (than the icosahedral) $C_{60}H_{60}$ fullerene structures of relatively high D_{5d} symmetry with ten endohydral hydrogens. The structure(s) with 20 (out of 60) endohydral hydrogen atoms become unstable and disjoint, leading (by bringing together the disjoint pieces) to stable "nanotubes" and fullerene structures, which can serve as good and transparent (building) models of larger nanotubes. The IR spectra of the derived fullerenes and nanotubes are compatible (within the uncertainties of the calculations) with the observed unidentified IR astronomical features. Therefore it would be possible that such structures (including partially hydrogenated fullerenes) could coexist in stellar atmospheres and could be responsible for the observed stellar IR features.

[1] A. Webster, Nature (London) **352**, 412 (1991).
[2] M. I. Attalla, A. M. Vassallo, B. N. Tattam, and J. V. Hanna, J. Phys. Chem. **97**, 6329 (1993).
[3] J. Nossal, R. K. Saini, L. B. Alemany, M. Meier, and W. E. Billups, Eur. J. Inorg. Chem. **2001**, 4167 (2001).
[4] B. S. Hudson, D. A. Braden, S. F. Parker, and H. Prinzbach, Angew. Chem., Int. Ed. **39**, 514 (2000).
[5] P. E. Eaton and T. W. Cole, Jr., J. Am. Chem. Soc. **86**, 962 (1964).
[6] (a) M. Saunders, Science **253**, 330 (1991); (b) P. W. Fowler, H. W. Kroto, R. Taylor, and D. R. M. Walton, J. Chem. Soc., Faraday Trans. **87**, 2685 (1991); (c) D. Bakowies and W. Thiel, Chem. Phys. Lett. **192**, 236 (1992).
[7] P. J. Stephens, F. J. Devlin, C. F. Chabalowski, and M. J. Frisch, J. Phys. Chem. **98**, 11623 (1994).
[8] TURBOMOLE (Version 5.6) (Universitat Karlsruhe, 2000).
[9] A. Schäfer, C. Huber, and R. Ahlrichs, J. Chem. Phys. **100**, 5829 (1994).
[10] M. Linnolahti, A. J. Karttunen, and T. A. Pakkanen, ChemPhysChem **7**, 1661 (2006).
[11] T. Yildirim, O. Gülseren, and S. Ciraci, Phys. Rev. B **64**, 075404 (2001).
[12] L. D. Book and G. E. Scuseria, J. Phys. Chem. **98**, 4283 (1994).
[13] A. D. Zdetsis, E. N. Koukaras, and C. S. Garoufalis, Appl. Phys. Lett. **91**, 203112 (2007).
[14] A. P. Scott and L. Radom, J. Phys. Chem. **100**, 16502 (1996); M. W. Wong, Chem. Phys. Lett. **256**, 391 (1996).